NJC

Accepted Manuscript

This article can be cited before page numbers have been issued, to do this please use: S. Y. Ebrahimipour, I. Sheikhshoie, J. simpson, H. ebrahimnejad, M. dusek, N. kharazmi and V. eigner, *New J. Chem.*, 2016, DOI: 10.1039/C5NJ02594J.

View Article Online
DOI: 10.1039/C5NJ02594J

Antimicrobial activity of arylhydrazone-based oxido vanadium(V) complexes: *in-vitro* and *in silico* studies

S. Yousef Ebrahimipour[a,*], Iran Sheikhshoaie[a], Jim Simpson[b], Hadi Ebrahimnejad[c], Michal Dusek[d], Nima Kharazmi[a], Vaclav Eigner[d]

[a] Department of Chemistry, Faculty of Science, Shahid Bahonar University of Kerman, Kerman, Iran

[b] Department of Chemistry, University of Otago, PO Box 56, Dunedin 9054, New Zealand

[c] Department of Veterinary Medicine, Shahid Bahonar University of Kerman, Kerman, Iran

[d] Institute of Physics ASCR, v.v.i., Na Slovance 2, 182 21 Praha 8, Czech Republic

* Corresponding author:

Dr. S. Yousef Ebrahimipour
Department of Chemistry, Faculty of Science
Shahid Bahonar University of Kerman, 76169-14111 Kerman, Iran.
Tel./fax: +98 34 3132 2143
Email: ebrahimipour@uk.ac.ir, Ebrahimipour@ymail.com

View Article Online
DOI: 10.1039/C5NJ02594J

Abstract

A tridentate Schiff base ligand (E)-N'-((2-hydroxynaphthalen-1-yl)methylene)benzohydrazide (**H_2L**) and its oxido-vanadium(V) complexes with formulae [VO(L)(MeOH)(OMe)] (**1**), [VO(L)(OEt)] (**2**), and [VO(L)(OPr)] (**3**) have been synthesized and fully characterized by physicochemical and spectroscopic methods including elemental analysis, FT-IR, ^{1}HNMR and molar conductivity. The solid state structures of **H_2L** and complexes **1-3** have been also investigated using single crystal X-ray analysis. It was concluded that **H_2L** crystallized in keto form in solid state, however in all complexes, the ligand appears in the enol form. The coordination geometry of complex **1** was found to be distorted octahedral while complexes **2** and **3** adopt a square pyramidal geometries. The antimicrobial activity of these compounds was also evaluated against *Escherichia coli* (ATCC 25922) and *Staphylococcus aureus* (ATCC 33591 and 29213) bacteria and the results showed that all three complexes have significant antibacterial activities. In order to determine the potential of these complexes as antimicrobial agents, molecular docking of the complexes with GlcN-6-P synthase was also investigated.

Keywords: Schiff base, Oxido-vanadium(V) complex, antimicrobial activity, X-ray crystal structure

View Article Online
DOI: 10.1039/C5NJ02594J

1. Introduction

Hydrazone-based Schiff base ligands have received considerable attention due to the ease with which they are synthesised and their wide range of applications. [1, 2] Schiff bases can coordinate a wide variety of transition metal ions in different oxidation states forming complexes with interesting properties, architectures and applications. [3, 4] Among the transition metals, vanadium has attracted considerable attention due to its important role in bioinorganic chemistry as well as in other fields. [5] For the different oxidation states of vanadium, only V(III), V(IV), and V(V) are involved in physiological systems. [6] As a biocompatible element, vanadium has a wide variety of biochemical and physiological functions. [7] Many of these are due to the inhibition or stimulation of enzymes that participate in phosphate metabolism.

A variety of different enzymes, including nitrogenases, haloperoxidases, [8, 9] phosphate-metabolizing enzymes [10] and phosphomutases [11], involve vanadium. Furthermore, vanadium is able to replace other transition metal ions in enzymes due to its compatibility with a variety of potential ligand systems. In addition, vanadium complexes are well documented to have therapeutic applications [12] and have also been used as model compounds to clarify the mechanisms of several biochemical processes. [13, 14]

One of the most interesting properties of metal complexes, including those of vanadium, is their antimicrobial activity. [15] Various methods have been reported to evaluate this activity. Glucosamine-6-phosphate synthase (GlcN-6-P synthase) has been recently considered as a new target in antimicrobial studies because the GlcN-6-P produced by this enzyme is crucial for the survival of the cell. [16, 17] It has been demonstrated that inactivation of GlcN-6-P synthase, even for a short-time, results in morphological changes, agglutination and lysis and is therefore lethal for pathogenic microorganisms. [18]

Any compounds that can inhibit the action of this enzyme is a potential antimicrobial agent. Molecular docking procedures provide important insights into the binding mechanism, affinity and potential activity of drug candidates such as metal complexes with protein targets such as GlcN-6-P synthase. [19]

In a continuation of our search for biologically potent molecules [15, 20-22], a tridentate hydrazine-based ligand (E)-N'-((2-hydroxynaphthalen-1-yl)methylene)benzohydrazide (**H_2L**) and three of its oxido-vanadium(V) complexes, [VO(L)(MeOH)(OMe)] (**1**) and [VO(L)(OR)] R = Et, (**2**); Pr, (**3**) have been synthesized and fully characterized. The antimicrobial activities of these

View Article Online
DOI: 10.1039/C5NJ02594J

compounds are also investigated against various microorganisms. Molecular docking studies were also performed in order to gain a better understanding of the drug-receptor interactions with these complexes.

2. Results and discussion

During the reaction of the ligand H_2L with the same equivalent of $[V^{(IV)}O(acac)_2]$ in alcoholic solvent (ROH; R=CH_3, C_2H_5, C_3H_7) under ambient conditions, V(IV) center is oxidized to V(V). Moreover, the coordinated acac molecules are replaced by the ligand and corresponding alkoxy groups resulted in the production of [V(V)O(OMe)(MeOH)(L)] or [V(V)O(OR)(L)] (R=C_2H_5 or C_3H_7). Here, the ligand acts as an ONO tridentate coordinating agent through its N–imine and O–phenolate moieties. The resulting complexes were stable in air. They are soluble in most common organic solvents except n-hexane and diethyl ether. Prior to complexation, the ligand adopts the enol tautomeric form and is doubly deprotonated to give the (1*Z*,N'*E*)-*N*'-(2-oxidonaphthalen-1-yl)methylenebenzohydrazonate dianion (Scheme 1). The molar conductivities of the complexes are in the range of 2.7-3.1 Ω^{-1} cm^2 mol^{-1} which confirms their behaviour as non-electrolytes. [23]

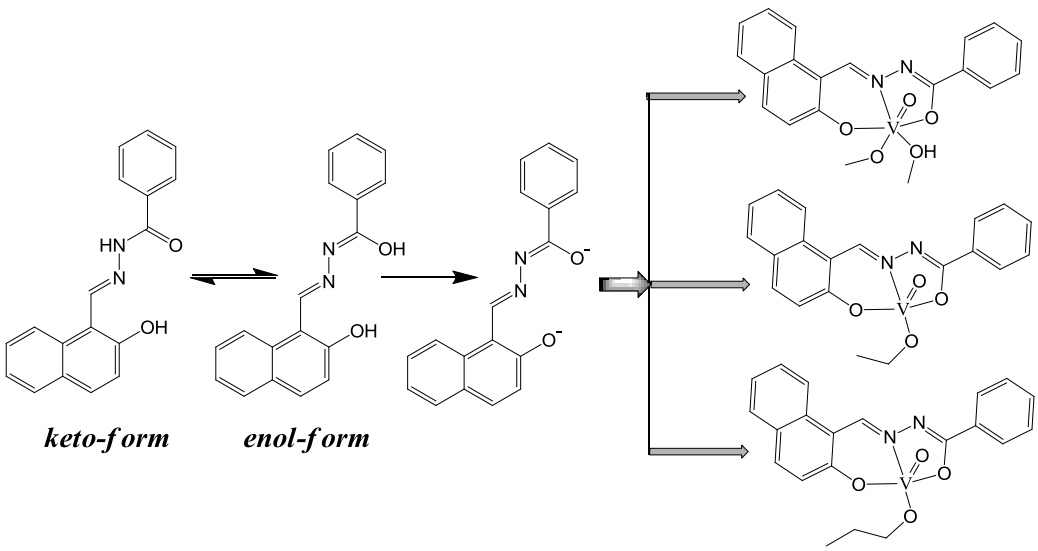

Scheme 1: schematic diagram of the complexation process.

2.1 Spectral characterizations

The infrared spectrum of the ligand displays absorption bands at 3297 and 1623 cm^{-1} assigned to NH and C=O vibrations respectively. Absence of these vibrations in the spectra of the complexes

View Article Online
DOI: 10.1039/C5NJ02594J

confirms that, while the uncomplexed ligand favours the *keto*-tautomer in the solid state, it adopts the *enol*-form prior to deprotonation and coordination. In the spectrum of **H_2L**, stretching and out of plane bending vibrations of the OH group appear at 3395 and 698 cm^{-1} respectively. [21] Disappearance of these peaks upon complexation (for **2** and **3**), confirms the coordination of the deprotonated phenolic oxygen to vanadium. In the ligand, the intense band at 1601 cm^{-1} is can be assigned to the stretching vibration of azomethine moiety. In the complexes however, these bands shift to lower wave number by 5, 3 and 7 cm^{-1} for **1** , **2** and **3** respectively [24]. These shifts imply the coordination of the azomethine nitrogen to the vanadium atom in complexes. The *ca*. 34 cm^{-1} reduction in wavenumber of the ν(C-O) vibration in the spectra of the complexes, is evidence for coordination of the phenolic oxygen to the central metal atom. [25] The characteristic V=O vibrations in the complexes are found as sharp peaks in the range 971-974 cm^{-1} . [26]The ^{1}HNMR spectra of the compounds were recorded in DMSO-d_6 at the ambient temperature. The spectrum of **H_2L** shows a singlet at 12.8 ppm for the OH proton resonance [27]. Disappearance of this peak in the spectra of the complexes confirms coordination of the deprotonated phenolic oxygen to the central metal atom.[21] In **H_2L**, a singlet at 12.2 ppm was assigned to the NH proton.[28] The absence of this peak in the specta of the complexes again provides a strong evidence for the adoption of the enol form of ligand in the complexes. The exchangeability of this proton in the ligand was confirmed by addition of D_2O to the DMSO-d_6 solution. In the spectra of complexes, the azomethine signal shows a significant downfield in comparison to the free ligand, supporting the fact azomethine nitrogen is bound to the vanadium atom. [4,22] The protons of the aromatic rings lie between in 7.2-8.4 ppm as multiplet signals. [4] ^{1}H NMR spectra of **1** and **2** in solution of DMSO-d_6 are almost identical to each other, except for the proton signals of the alkoxide chain,. In the ^{1}HNMR of [VO(L)(MeOH)(OMe)], **1**, the signal for methyl group of the coordinated methanol molecule and of the methoxy group both appear at 3.1 ppm. The hydroxyl resonance proton of coordinated methanol can be found at 5.3 ppm. In spectrum of **2**, the CH_2 and CH_3 resonances of the ethyl group of the ethoxide appear at 3.4 ppm as a quartet and 1.1 ppm as a triplet respectively. In the case of **3**, the protons of the propoxide ligand resonate in the classic triplet, multiplet, triplet pattern with peaks at 3.3 ppm $OC\underline{H}_2$, 1.4 ppm $OCH_2C\underline{H}_2$ and 0.8 ppm, $C\underline{H}_3$.

2.2 X-ray structure determinations

View Article Online
DOI: 10.1039/C5NJ02594J

Selected bond distances and angles for **H_2L** and the complexes **1-3** are listed in Table 1. The structure of the free ligand molecule is shown in Fig. 1 and clearly reveals the adoption of the *keto*-tautomeric form in the solid state with C12=O2 = 1.2324(16) Å, N2—C12 = 1.3523(19) Å and the hydrogen atom on N2 readily located in a difference Fourier map and refined with a restrained bond length N2—H1n2 of 0.920(9) Å.

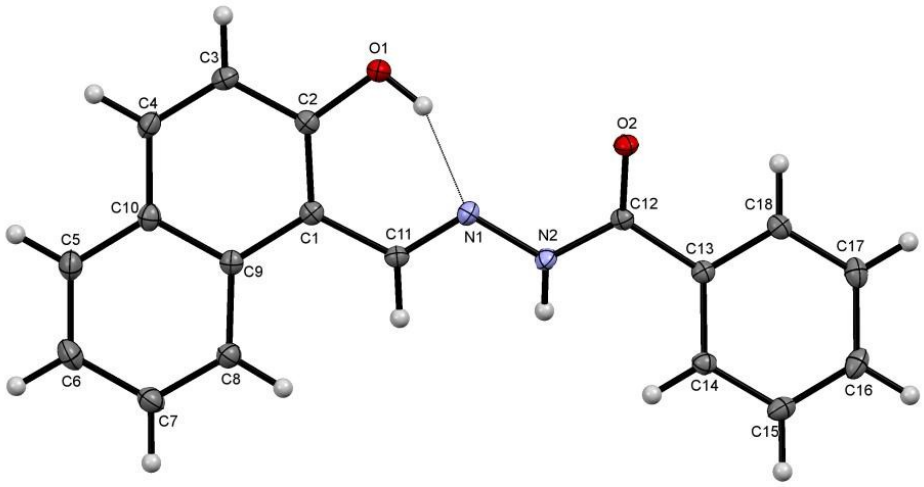

Fig. 1. The molecular structure of **H_2L** showing the atom numbering scheme with ellipsoids drawn at the 50% probability level. An intramolecular hydrogen bond is drawn as a dotted line.

The entire molecule is not completely planar with an *rms* deviation of 0.2373 Å from the best fit plane through all 22 non-hydrogen atoms. This is despite the intramolecular hydrogen bond formed between the hydroxyl substituent on the naphthalene ring and the N1 atom, Fig. 1, Table 2. The central C11, N1, N2, C12, O2 portion of the molecule is certainly planar, *rms* deviation 0.0365 Å, and subtends angles of 18.22(3)° and 31.46° respectively to the naphthalene (C1…C10) and phenyl (C13…C18) ring systems. Bond distances and angles in the molecule are not unusual [29] and agree well with those found in the structure of a hydrate of the same molecule [30].

View Article Online
DOI: 10.1039/C5NJ02594J

Table 1. Selected bond lengths, (Å), and angles, (°), for **H_2L** and complexes **1, 2 and 3**.

	H_2L	**1**	**2**	**3**
V1—O1v		1.5926(10)	1.582(3)	1.586(2)
V1—O1		1.8704(10)	1.856(2)	1.8501(19)
V1—O2		1.9675(10)	1.927(3)	1.933(2)
V1—N1		2.1158(10)	2.094(3)	2.091(2)
V1—O3		1.7790(9)	1.752(2)	1.748(2)
V1—O4		2.2832(10)		
O1—C2	1.3505(18)	1.3309(15)	1.335(4)	1.335(3)
C1—C11	1.455(2)	1.439(2)	1.435(5)	1.428(4)
C11—N1	1.2857(19)	1.2971(16)	1.297(4)	1.301(4)
N1—N2	1.3815(18)	1.3944(16)	1.392(4)	1.389(3)
N2—C12	1.3524(19)	1.3165(15)	1.311(4)	1.303(4)
C12—O2	1.2324(16)	1.2999(15)	1.306(4)	1.308(3)
C12—C13	1.491(2)	1.4826(19)	1.472(5)	1.477(4)
O4—C22		1.402(2)		
O4—C22'		1.400(3)		
O1v—V1—O1		99.15(5)	105.10(13)	105.96(10)
O1v—V1—O2		97.66(5)	103.85(13)	103.30(10)
O1v—V1—O3		101.87(4)	109.02(14)	109.22(10)
O1v—V1—N1		94.77(4)	98.88(13)	98.58(10)
O1v—V1—O4		174.90(5)		
O1—V1—O2		152.43(4)	144.89(13)	144.75(8)
O1—V1—O3		101.84(4)	98.11(12)	98.87(9)
O1—V1—N1		82.43(4)	82.03(11)	82.26(8)
O1—V1—O4		82.72(4)		
O2—V1—O3		95.87(4)	90.79(12)	89.55(9)
O2—V1—N1		74.52(4)	74.24(11)	74.29(8)
O2—V1—O4		78.70(4)		
O3—V1—N1		161.84(5)	150.89(14)	150.50(9)
O3—V1—O4		82.28(4)		

View Article Online
DOI: 10.1039/C5NJ02594J

Table 2. Hydrogen bond distances (Å), angles (°) for **H_2L** and complexes 1-3.

Compound	D—H…A	D—H	H…A	D…A or	‹ D—H…A
H_2L	O1—H1o1…N12	0.860(13)	1.778(11)	2.5652(17)	149(2)
	N2—H1n2…O2$^{L(i)}$	0.920(9)	1.941(11)	2.8345(15)	163.2(13)
	C11—H1c11…O2$^{L(i)}$	0.96	2.54	3.2523(18)	132
	C14—H1c14…O1$^{L(ii)}$	0.96	2.46	3.360(2)	156
	C15—H1c15…O2$^{L(ii)}$	0.96	2.70	3.4456(19)	136
1	O4—H1o4…N2$^{1(i)}$	0.860(5)	1.915(4)	2.7718(14)	173.7(16)
	C5—H1c5…O1v$^{1(ii)}$	0.96	2.42	3.3740(19)	173
	C7—H1c7…O2$^{U1iii)}$	0.96	2.51	3.453(2)	171
	C14—H1c14…O4 $^{1(i)}$	0.96	2.71	3.422(2)	132
	C3—H1c3…Cg4$^{1(ii)}$	0.96	2.94	3.775(2)	148
	C4—H1c4…Cg3 $^{1(ii)}$	0.96	2.97	3.7263(19)	137
2	C3—H1c3…O1V$^{2(ii)}$	0.96	2.61	3.527(5)	163
	C19—H1c19…O1V$^{2(iii)}$	0.96	2.68	3.244(6)	116
	C4—H1c4…Cg5$^{2(iv)}$	0.96	2.65	3.417(4)	137
	C8—H1c8…Cg4$^{2(v)}$	0.96	2.93	3.692(4)	137
	C16—H1c16…Cg3$^{2(vi)}$	0.96	2.71	3.472(4)	137
	C17—H1c17…Cg4$^{2(vi)}$	0.96	2.97	3.628(4)	127
3	C3—H1c3…O1V$^{3(ii)}$	0.96	2.66	3.582(4)	164
	C19—H1c19… O1V$^{W(iii)}$	0.96	2.70	3.57(2)	147
	C4—H1c4…Cg5$^{3(iv)}$	0.96	2.65	3.428(3)	139
	C8—H1c8…Cg4$^{3(v)}$	0.96	2.93	3.684(3)	137
	C15—H1c15…Cg4$^{3(vi)}$	0.96	2.95	3.595(3)	126
	C16—H1c16…Cg3$^{3(vi)}$	0.96	2.65	3.426(3)	138

Symmetry codes: L(i) x+1/2, −y+1/2, z+1/2; L(ii) x, y, z+1; 1(i) −x+1, −y+2, −z; 1(ii) −x+3/2, y+1/2, −z−1/2; 1(iii) x−1/2, −y+3/2, z−1/2; 2(ii) x, y−1, z; 2(iii) −x+1, −y+1, −z. 2(iv) x, −y−1/2, z−1/2; 2(v) −x+2, y+1/2, −z+1/2; 2(vi) x, −y+1/2, z−3/2; 3(ii) x, y−1, z; 3(iii) −x+2, y, −z+1/2; 3(iv) −x+1/2, y+1/2, −z+1/2; 3(v) x+1, −y, z−1/2; 3(vi) −x+1/2, y+3/2, −z−1/2.Cg3, Cg4 and Cg5 are the centroids of the C1, C2, C3, C4, C9, C10; C5, C6, C7, C8, C9, C10 and C13, C14, C15, C16, C17, C18 rings respectively.

The Cambridge Structural Database, CSD [31], also reveals 20 closely related molecules with a wide variety of different substituents on the benzene ring. These include the *m*- and *p*-tolyl derivatives [32] and an unusual bis(2-hydroxy-1-naphthaldehyde)-1,3-benzenedicarbohydrazone [33],

View Article Online
DOI: 10.1039/C5NJ02594J

with two 2-hydroxynapthaldehyde units as substituents on the benzene ring. Crystal packing in the ligand is stabilised by one classical N—H…O and three non-classical C—H…O hydrogen bonds Table 2. A reasonably strong offset π…π stacking interaction also occurs between the phenyl ring and the hydroxyl substituted ring of the naphthalene system with a centroid to centroid distance of 3.6412(9) Å. [34] This is augmented by a second π…π contact between the C=N double bond and the phenyl ring at a distance of 3.440(1) Å and these contacts combine to stack the molecules along the *a* axis direction, Fig S1.

In the V(V) complex, [VO(L)(MeOH)(OMe)], the oxovanadium(V) cation is coordinated to the doubly deprotonated tridentate L^{-2} ligand and a methoxide anion but there is also an additional coordination site occupied by a neutral methanol molecule, rendering the V atom six-coordinate Fig. 2.

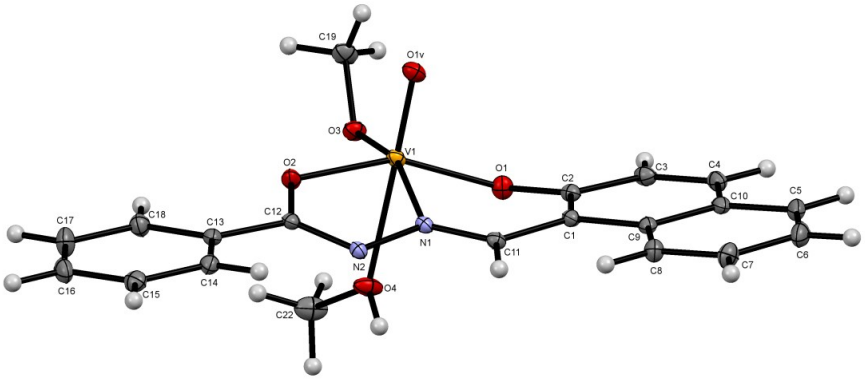

Fig. 2. The molecular structure of [VO(L)(MeOH)(OMe)] showing the atom numbering scheme with ellipsoids drawn at the 50% probability level. For clarity, only the major disorder component of the methyl group of the methanol ligand is shown.

This structure has been briefly reported previously [35], from data collected at ambient temperature, but is included in the discussion here for completeness and to allow comparisons of both its molecular and crystal structures with those of complexes **2** and **3**. The coordination geometry of the V(V) atom is distorted octahedral with the equatorial plane occupied by the O1, N1, O2 and O3 atoms with an *rms* deviation of 0.0079 Å from that plane. The V1 atom lies 0.2908(8) Å out of this plane in the direction of O1V with the second axial site occupied by the O4 atom of the additional methanol ligand. V=O (O_4N) complexes abound with 285 hits on the

View Article Online
DOI: 10.1039/C5NJ02594J

CSD. However, in addition to the previous report [35], only four other structures containing variants of the 2-oxidonaphthalen-1-yl)methylenebenzo-hydrazonateligand are found. [36]

Crystal packing for [VO(L)(MeOH)(OMe)] differs significantly from that for [VO(L)(OEt)] and [VO(L)(OPr)]. In particular, the presence of the additional methanol ligand occupying the sixth position in the coordination sphere of the metal obviates any close contact between the metal atom and any of the aromatic rings. Classical O4—H1o4…N2 hydrogen bonds form inversion dimers and generate $R^2_2(10)$ rings. These contacts are strengthened by both C14-H1c14…O4 hydrogen bonds and offset π…π stacking interactions between the phenyl ring and the O1 bound ring of the naphthalene ring system, Fig. 3, with Cg3…Cg5 = 3.6359(12) Å (Cg3 and Cg5 are the centroids of the C1, C2, C3, C4, C9, C10 and C14…C19 rings respectively).

In addition C—H…O and C—H…π contacts, Table 2, further stabilise the structure and these interactions combine to generate a three-dimensional network of molecules stacked along the *b* axis direction, Fig S2.

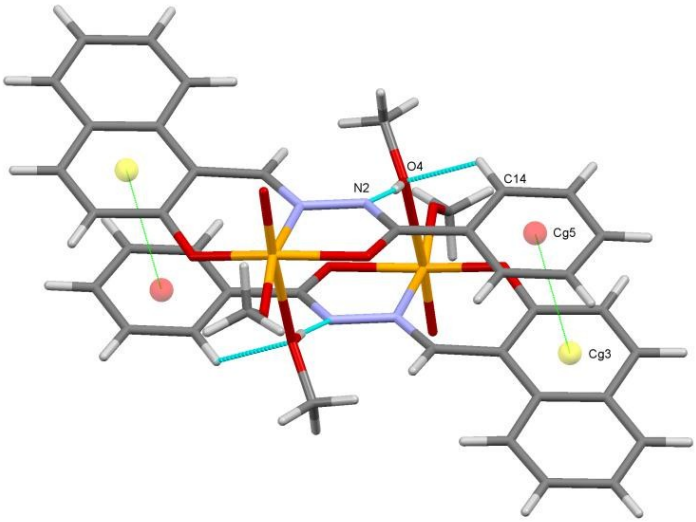

Fig.3.Inversion dimers of [VO(L)(MeOH)(OMe)]. π …π contacts are shown as green dotted lines with ring centroids represented by coloured spheres.

The molecular structures of the two five-coordinate vanadium(V) complexes, **2** and **3** reported here, Fig. 4 and Fig. 5 are sufficiently similar to be discussed together.

View Article Online
DOI: 10.1039/C5NJ02594J

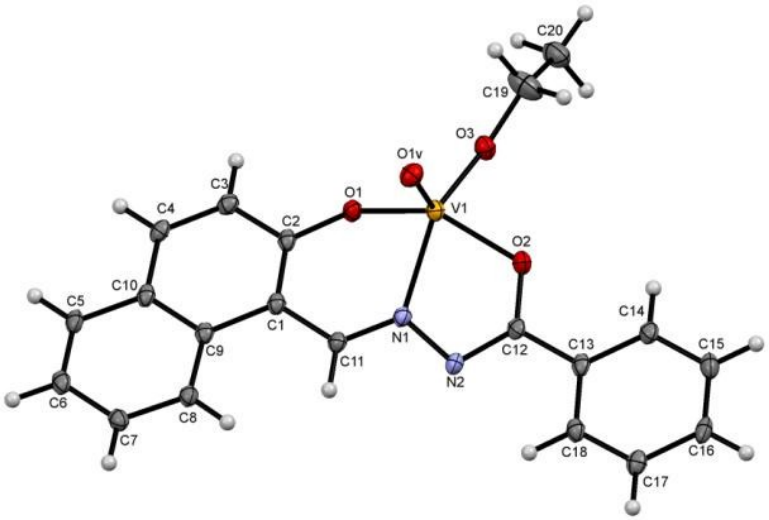

Fig. 4.The molecular structure of [VO(L)(OEt)] showing the atom numbering scheme with ellipsoids drawn at the 50% probability level.

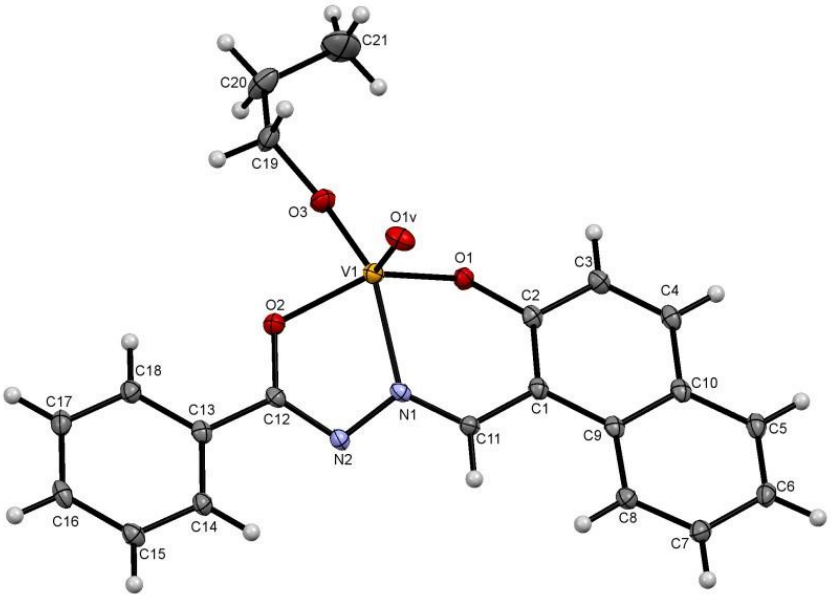

Fig. 5. The molecular structure of [VO(L)(OPr)] showing the atom numbering scheme with ellipsoids drawn at the 50% probability level. For clarity, only the major disorder component in the alkyl chain of the propoxide ligand is shown

They differ only in the nature of the alkoxide, either ethoxide, **2**, or propoxide, **3**, that acts as the third anionic ligand species. Both complexes comprise an oxovanadium(V) cation in a slightly distorted square pyramidal coordination environment bound to the two O atoms and the N1

View Article Online
DOI: 10.1039/C5NJ02594J

hydrazone atom of the doubly deprotonated (2-oxidonaphthalen-1-yl)methylenebenzohydrazonate dianion. The fifth coordination site is occupied by the O atoms of ethoxide for **2** or propoxide for **3**. The hydrazonate and alkoxide ligands lie in the square plane with the oxido, O1v, atoms axial with the O1 and O2 or O3 and N1 atoms mutually *trans* in each case. The best fit equatorial plane through the four ligand donor atoms has an *rms* deviation of 0.0160 Å with the V1 atom lying 0.4765 (15) Å out of that plane in the direction of O1v. The corresponding plane for **3** has an *rms* deviation of 0.0192 Å with V1 out of the plane by 0.2915(10) Å in the same direction. The extent of distortion from trigonal bipyramidal geometry can be determined by calculating the trigonality index, τ_5, described by Addison *et al* [37]. τ_5 = 0 for an ideal square–pyramid and τ_5 = 1 for an ideal trigonal bipyramid. For **2**, τ_5 = 0.099 while for **3**τ_5 = 0.096 confirming that both complexes can quite reasonably be described as square pyramidal with only minimal distortion. Five coordinate VO^{3+} complexes with a V=O(O_3N) coordination sphere are again quite common registering 181 hits on the CSD . However, narrowing the search to include a tridentate ligand similar to **H_2L** shows only two closely related complexes, (N-(1-(2-(hydroxy)-1-naphthyl)ethylidene)-4-methylbenzenecarbohydrazonato)-methoxo-oxo-vanadium(V) [36b] and *cis*-dioxo-(2-hydroxy-1-naphthaldehyde isonicotinylhydrazone)-vanadium(V) trihydrate [38].

Comparison of equivalent bond distances in the coordination spheres of these related complexes show that the V=O (1.596 and 1.629 Å) and V—N (2.186 and 2.120) Å distances are considerably longer than those reported here, Table 1; the variation would seem to be too great to be explained simply by the fact that these data for these two related structures were obtained at ambient temperature.

In the crystal structure of **2** C4—H1c4…Cg5 contacts link molecule into rows in an obverse fashion along *c*. These rows are interconnected by C19—H1c19…O1v hydrogen bonds that form inversion dimers and generate $R^2_2(10)$ rings, Fig 6(a), Table 2 [39], forming layers of molecules in the *ac* plane. There are clear similarities between the crystal packing of **2** and **3**. For **3**, inversion dimers also form through C19—H1c19…O1v contacts, although in this case the dimers are linked into parallel chains along *c* by C4—H1c4…Cg5 contacts, also generating layers of molecules in the *ac* plane, Fig. 6(b).

View Article Online
DOI: 10.1039/C5NJ02594J

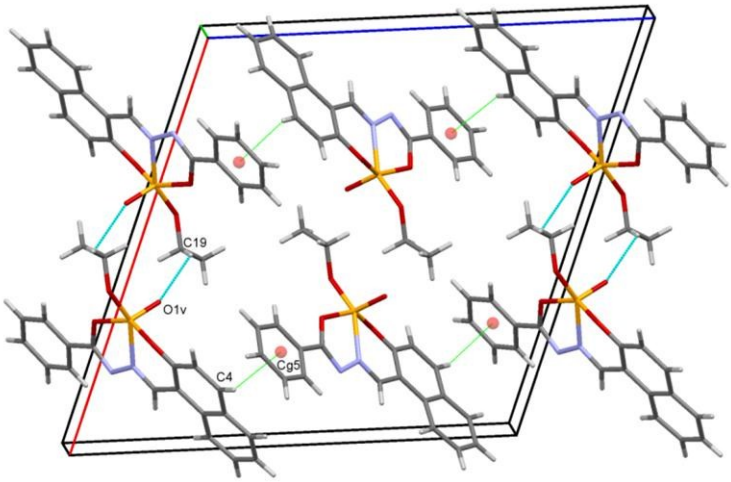

(a)

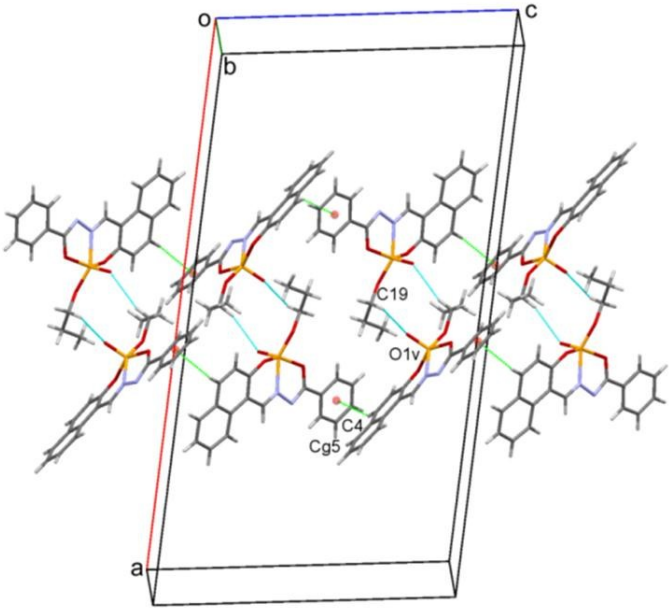

(b)

Fig. 6. Layers of molecules of (a) complex **2** and (b) **3**. In these and subsequent Figures, hydrogen bonds are drawn as dashed lines. C—H…π contacts are shown as green dotted lines with ring centroids represented by coloured spheres.

A second series of C3—H1c3…O1v hydrogen bonds link molecules of complex **2** into C(6) chains [39] along *b*. Interestingly, these C—H…O hydrogen bonds are seemingly augmented by an

View Article Online
DOI: 10.1039/C5NJ02594J

unusually close ring to metal interaction Cg5…V1[2i] at a distance of 3.797 Å (2i = x,y+1,z) shown in Fig. 7(a).

A closely similar situation exists for complex **3**, again with the C3—H1c3…O1v derived C(6) chain along *b* bolstered by an almost identical Cg5…V1[3i] contact at a distance of 3.793 Å [31] (3i = x,y+1,z), Fig. 7(b) Such contacts, while presumably weak, are not unprecedented and are related to the cation…π interactions that have previously been suggested to contribute to the overall stabilisation of structures in both small molecule and protein systems [40].

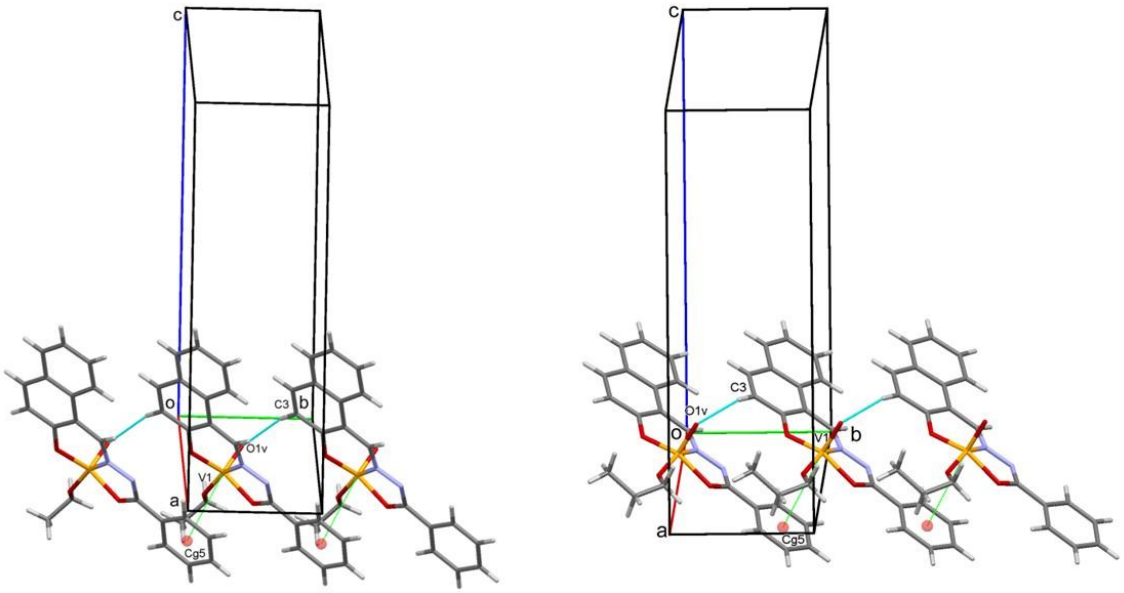

Fig. 7. C(6) chains of molecules of (a) [VO(L)(OEt)] and (b) [VO(L)(OPr)] along *b*. The unusual V…π contacts are shown as green dashed lines.

Similar close contacts have also been observed in the crystal structures of other transition metal complexes where the metal presents with a vacant coordination site [21, 41,42]. Interestingly, the database reveals six similar close V…π contacts in square pyramidal V(V) complexes with VO_4N coordination spheres with metal…centroid distances under 4.0 Å [43-46]. However, the possibility or potential significance of such contacts is not mentioned in the reports of these related structures. In these other examples, the V…centroid distances lie in the range 3.859 to 3.967 Å, suggesting that the contact observed here is relatively strong.

Chains of molecules of complex **2** also form along *c* as a result of C16—H1c16…Cg3 and C17—H1c17…Cg4 contacts, Fig. 8a, while C16—H1c16…Cg3 and C17—H1c15…Cg4

View Article Online
DOI: 10.1039/C5NJ02594J

contacts also form chains of complex **3** molecules also along *c*, Fig. 8b. These contacts combine with the previously described interactions to generate an extensive three dimensional network of molecules stacked along the *b* axis direction (Figs. S3 and S4).

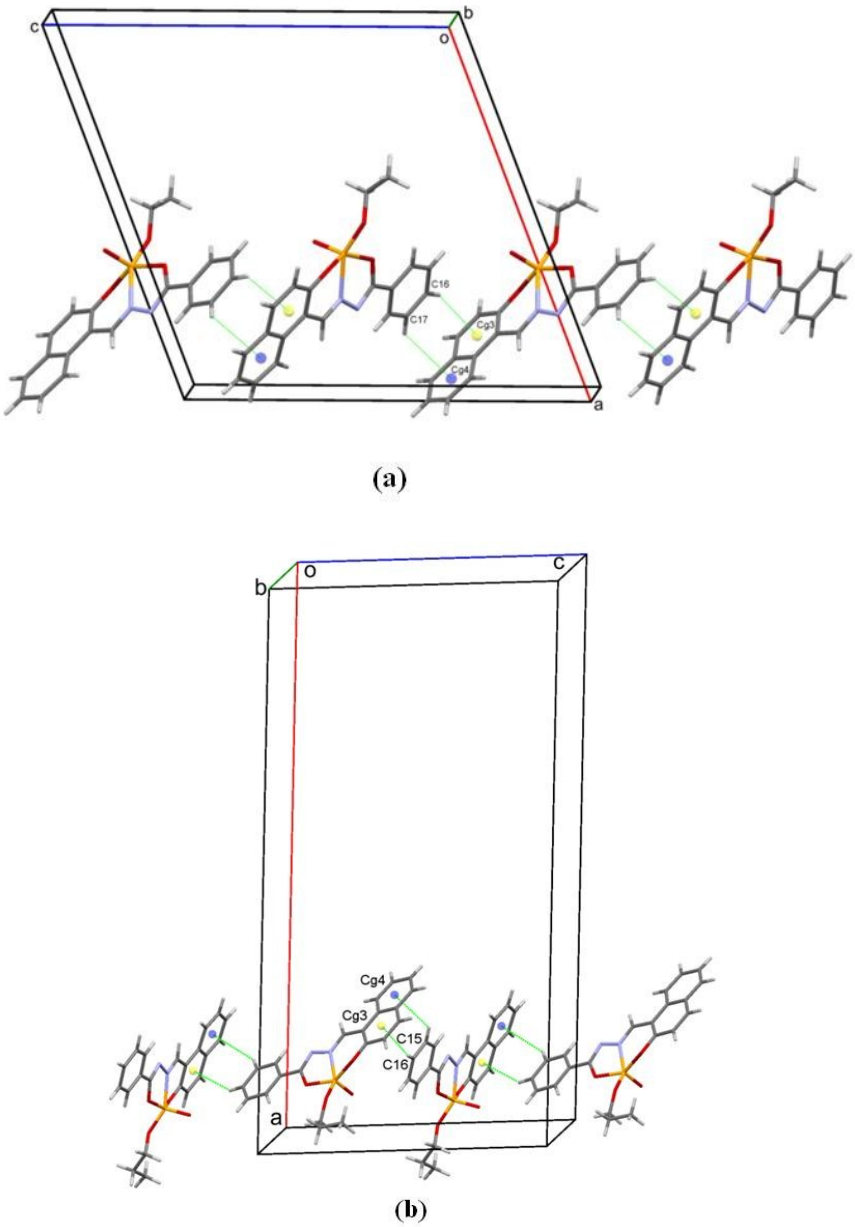

Fig. 8. Additional C—H…π chains of molecules of (a) [VO(L)(OEt)] and (b) [VO(L)(OPr)] along the c axis direction.

View Article Online
DOI: 10.1039/C5NJ02594J

2.3 Antibacterial activity

Table 3 shows the MIC ranges of the ligand and the complexes; [VO(L)(MeOH)(OMe)], [VO(L)(OEt)] and [[VO(L)(OPr)] against gram-positive (*Staphylococcus aureus*) and gram-negative (*Escherichia coli*) bacteria generated by agar dilution. Not surprisingly, the ligand (H2L) did not exhibit a distinct antimicrobial effect per se against *Staphylococcus aureus* (ATCC 33591 and 29213) and *Escherichia coli* (ATCC 25922) (MIC: 5000 μg mL^{-1} <) whereas its complexes demonstrated different antimicrobial properties against these bacteria.

Table 3. Minimum inhibitory concentration (MIC) of the compounds against gram-positive and gram-negative bacteria *via* the agar dilution method.

Compounds	minimum inhibitory concentration (μg mL^{-1})		
	Escherichia coli (ATCC 25922)	*Staphylococcus aureus* (ATCC29213)	*Staphylococcus aureus* (MRSA[1], ATCC 33591)
Ligand	5000<	5000<	5000<
1	<19.53	<19.53	<19.53
2	39.06	39.06	78.13
3	39.06	39.06	39.06
Negative control (DMSO)	-	-	-

[1] methicillin-resistant *Staphylococcus aureus*

Zone of antibacterial inhibition against *Escherichia coli* shown by [VO(L)(OEt)], determined by the agar well diffusion method is shown in fig. 9.

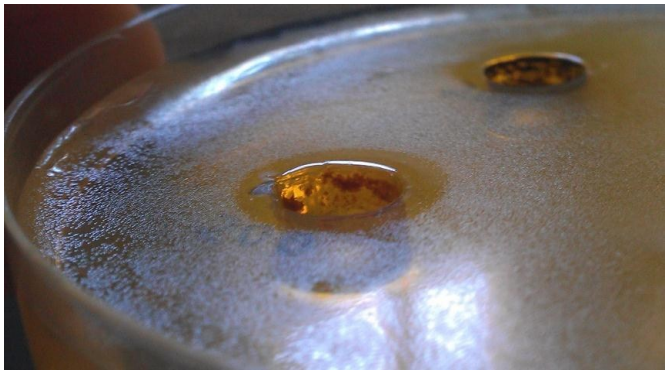

Fig. 9. Zone of antibacterial inhibition against *Escherichia coli* shown by [VO(L)(OEt)], determined by agar well diffusion method.

View Article Online
DOI: 10.1039/C5NJ02594J

Despite the resistance displayed by methicillin-resistant *S. aureus* (MRSA) against different antibiotics, the complexes [VO(L)(OEt)], [VO(L)(OPr)] and especially [VO(L)(MeOH)(OMe)], showed explicit anti-MRSA activity. Furthermore, [VO(L)(MeOH)(OMe)] inhibited the growth of *S. aureus* and *E. coli* at relatively low concentration, 19.53 µg mL^{-1}.

Antimicrobial activity of the compounds was also evaluated based on the diameters of the clear inhibition zones surrounding the wells. 500 and 1000 µg of complexes 1-3 provided effective inhibition of the growth of *S. aureus* (ATCC 29213 and 33591) and *E. coli* (ATCC 25922) (Table 4). Here, the anti-MRSA activity of 500 and 1000 µg of the [VO(L)(MeOH)(OMe)] was also associated with 28 and 30.5 millimeters of zone of inhibition respectively.

The higher activity of the metal complexes may be due to the changes occurred in the properties of the metal ions after chelation. According to Tweedy's chelation theory, polarity of the central metal ion reduces due to partial sharing of its positive charge with donor groups of ligands resulting in electron delocalization over the entire ring. Accordingly, penetration of the complexes into the lipid membranes will be improved and as will blockage of the metal-binding sites in the the enzymes of the microorganism [47].

Table 4. Antimicrobial activity of the compounds against gram-positive and gram-negative bacteria determined by the agar well diffusion method.

Bacteria	Compounds										
	3 (µg $well^{-1}$)		2 (µg $well^{-1}$)		1 (µg $well^{-1}$)		Ligand		Cefixime[a] (µg $well^{-1}$)	Azithromycin[b] (µg $well^{-1}$)	DMSO[c] (µL $well^{-1}$)
	1000	500	1000	500	1000	500	1000	500	5	15	100
Escherichia coli (ATCC 25922)	11.5	9	14	13	30	27	0	0	19.5	0	0
Staphylococcus aureus (ATCC 29213)	13	12	13	11.5	26	20	0	0	12.5	20	0
Staphylococcus aureus(MRSA, ATCC 33591)	7.5	7	12	11	30.5	28	0	0	12	15.5	0

a, b: Positive controls, c: Negative control

View Article Online
DOI: 10.1039/C5NJ02594J

2.4 Molecular docking studies

GlcN-6-P synthase was used as a target for the antimicrobial activity of complexes 1—3 as potential inhibitors. The orientation of the inhibitors bound to the active site of the enzyme was determined using automated docking. Binding energy and inhibition constants for all of the compounds together with those of the standard drugs Cefixime and Azithromycin for comparison are listed in Table 5.

Table 5. Binding energy (kcal mol^{-1}) and inhibition constant of the complexes **1-3**, cefixime and Azithromycin.

Compound	Binding energy (Kcal mol^{-1})	Inhibition constant (μM)
Complex 1	-5.33	123.33
Complex 2	-5.21	151.03
Complex 3	-5.19	157.32
Cefixime	-4.82	294.21
Azithromycin	-4.27	744.28

Docked images for title compounds and standard drugs are shown in Fig. 10. Docking of cefixime, azithromycin and the compounds synthesized here with the enzyme showed that all of the inhibitors can bind to one or more amino acids in the active site. In addition, the theoretical binding energies of the tested compounds were obtained in the range of -4.27 kcal/mol -5.33 kcal/mol respectively. Results obtained revealed that all of the vanadium complexes bind less strongly to GlcN-6-P synthase than the standards. However, for complex **1** a docking energy and a binding energy of -8.46 kcal/mol and -5.33 kcal/mol were obtained respectively suggesting that it may be a good inhibitor of GlcN-6-P synthase and subsequently a good antimicrobial agent.

View Article Online
DOI: 10.1039/C5NJ02594J

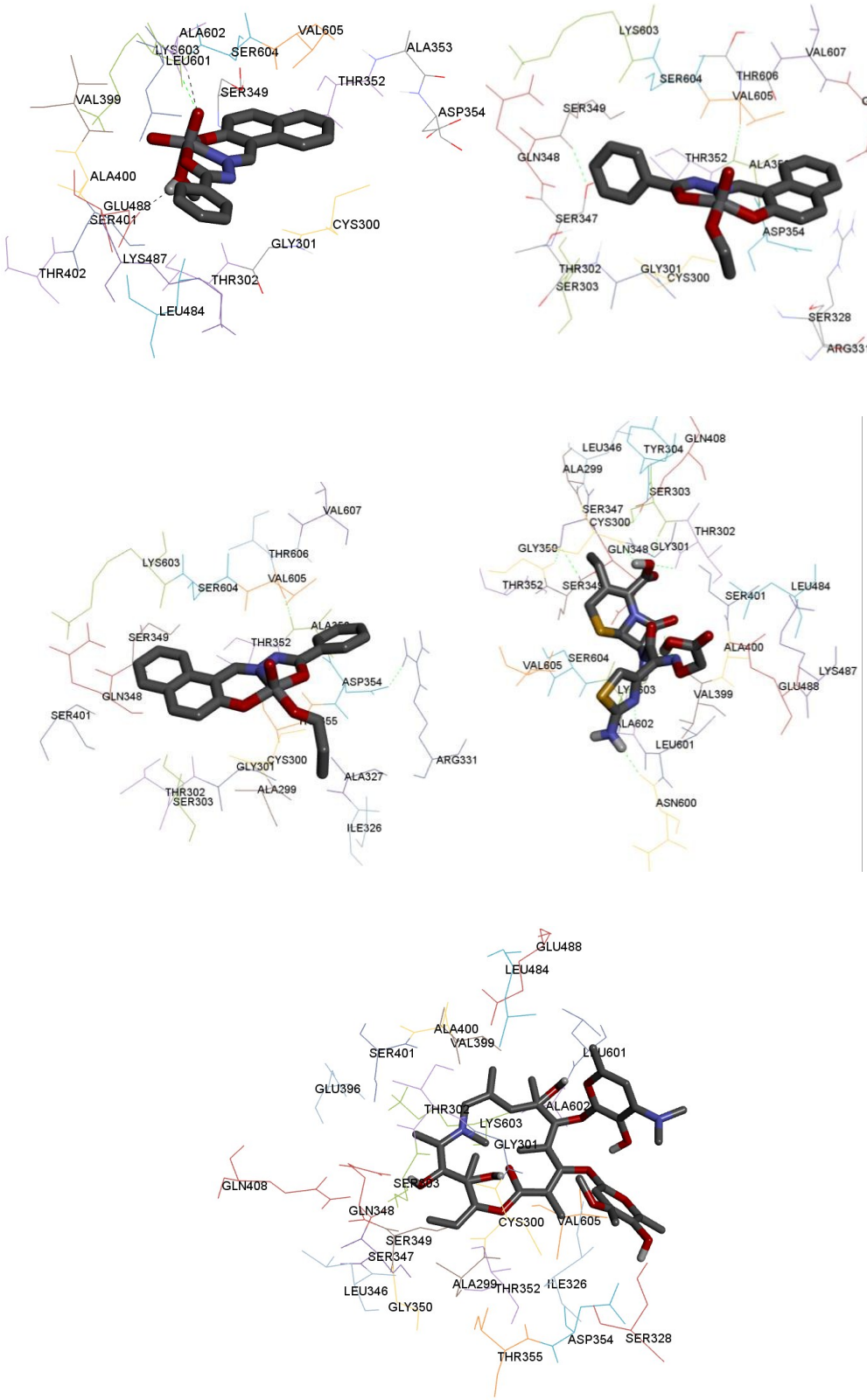

Fig 10. The docked complexes, cefixime and azitomycine in the active pocket of GlcN-6-P.

View Article Online
DOI: 10.1039/C5NJ02594J

3. Conclusion

Three oxido-vanadium(V) complexes have been prepared by the reaction of tridentate ligand **H_2L** and $VO(acac)_2$ in 1:1 molar ratio in appropriate solvents. All of the compounds were characterized by standard methods including X-ray crystal structure, FTIR, ^{1}HNMR, molar conductivity and elemental analysis. In all of the complexes the V(V) centre is coordinated to ONO donor atoms of the deprotonated Schiff base ligand, an oxo group and the oxygen donor(s) of alkoxide ligands and in one instance a coordinated methanol molecule. In-vitro antimicrobial activities of title compounds revealed that complexation enhanced the biological activities of the ligand. All three vanadium complexes showed an *in-vitro* antimicrobial characteristic to gram-positive and gram negative bacteria, particularly towards methicillin-resistant *S. aureus* that is resistant to numerous antibiotics. In particular [VO(L)(MeOH)(OMe)], showed explicit anti-MRSA activity and further *in vivo* or *in-situ* testing of these complexes are planned. Docking studies also suggested that complex **1**, with a minimum binding energy should be a good inhibitor of GlcN-6-P synthase.

4. Experimental

4.1 Materials and instrumentation

All chemicals and solvents used were of analytical reagent grade and were used as received. C, H, N microanalyses were determined on a Thermo Finnigan Flash Elemental Analyzer 1112EA. Melting points were measured on an Electrothermal-9100 apparatus and are uncorrected. FT-IR spectra were recorded on a FT-IR 8400-Shimadzu as KBr discs in the range 400-4000 cm^{-1}. Molar conductance measurements were made using a Metrohm 712 Conductometer in MeOH. ^{1}H-NMR spectra were recorded at 25 °C on a Bruker AVANCE 400 spectrometer.

4.1.1 Synthesis of (E)-N'-((2-hydroxynaphthalen-1-yl)methylene)benzohydrazide (H_2L)

An ethanolic solution (4 mL) of benzohydrazide (0.14 g, 1 mmol) was added dropwise to 4 mL of an ethanolic solution of 2- hydroxynaphthaldehyde (0.17 g, 1 mmol) with constant stirring.

View Article Online
DOI: 10.1039/C5NJ02594J

The yellow solution so obtained was left undisturbed at room temperature. Single crystals suitable for X-ray analysis appeared in the solution after 1 day; they were separated and dried in a desiccator over anhydrous $CaCl_2$.

Yield: 65%. m.p.: 156 °C. Anal. Calc. for $C_{18}H_{14}N_2O_2$ (290.32 g mol^{-1}): C, 74.47; H, 4.86; N, 9.65. Found: C, 74.38; H, 4.81; N, 9.63%. FT-IR (KBr) cm^{-1}: *v*(OH) 3395, *v*(NH) 3297, *v*(C=O) 1623, *v*(C=N) 1601, *v*($C=C_{ring}$) 1453, *v*(CO) 1351, *v*(NN) 1155.*v* (OH) 698. ^{1}H-NMR (400 MHz, DMSO-d_6, 25 ºC, ppm): δ = 12.8 (*s*, 1H; OH), 12.2 (*s*, 1H; NH), 9.50 (*s*, 1H; CH=N), 7.24 (*d*, *j*=8.9 Hz, 1H, Ar-H), 7.41 (*t*, *j*=7.4 Hz, 1H, Ar-H), 7.56-7.66 (*m*, 4H, Ar-H), 7.89(*d*, *j*=8.0 Hz, 1H, Ar-H), 7.93(*d*, *j*=9.0 Hz, 1H, Ar-H), 7.99 (*d*, *j*= 7.0 Hz, 2H, Ar-H), 8.22 (*d*, *j*=8.5 Hz, 1H, Ar-H)

4.1.2 Synthesis of the complexes 1-3

The three vanadium complexes were each prepared by the following method: 0.1 mmol of $VO(acac)_2$ (0.03 g) was added to equimolar quantities of **H_2L** (0.1 mmol, 0.03 g) in the appropriate solvent (methanol for **1** and ethanol and propanol for **2** and **3** respectively) and the resulting clear solution was refluxed for 10 min at 90°C. After cooling, the solution was left exposed to air and crystallization took place by slow evaporation at room temperature. After 2 days, single crystals suitable for X-ray diffraction were extracted and dried in a desiccator over anhydrous $CaCl_2$.

Methanol-(2-oxidonaphthalen-1-yl)methylene)benzohydrazonato-methoxido-oxido-vanadium(V) [VO(L)(MeOH)(OMe)] (1)

Yield: 65%. m.p.: >300 °C. Molar Conductance (10^{-3} M, MeOH): 3.1 Ω^{-1} cm^2 mol^{-1}. Anal. Calc. for $C_{20}H_{19}N_2O_5V$ (418.32 g mol^{-1}): C, 57.42; H, 4.58; N, 6.70. Found: C, 57.37; H, 4.51; N, 6.72%. IR (KBr) cm^{-1}: *v*(OH) 3442, *v*(C=N) 1596, *v*($C=C_{ring}$) 1441, *v*(C-O) 1289, *v*(NN) 1140, *v*(V=O)971, *v*(VO)558, *v*(VN)524. ^{1}H-NMR (400 MHz, DMSO-d_6, ppm): δ = 9.8 (*s*, 1H; *H*C=N), 7.2-8.4 (*m*, 11H; rings), 5.3 (*q*, 1H; O*H*), 3.1 (*m*, 6H; 2CH_3).

(2-oxidonaphthalen-1-yl)methylene)benzohydrazonato-ethoxido-oxido-vanadium(V) [VO(L)(OEt)] (2)

View Article Online
DOI: 10.1039/C5NJ02594J

Yield: 63%. m.p.: >300 °C. Molar Conductance (10^{-3} M, MeOH): 2.7 Ω^{-1} cm^2 mol^{-1}. Anal. Calc. for $C_{20}H_{17}N_2O_4V$ (400.30 g mol^{-1}): C, 60.01; H, 4.28; N, 7.00. Found: C, 60.09; H, 4.34; N, 6.93%. IR (KBr) cm^{-1}: *v*(C=N) 1598, *v*(C=C_{ring}) 1447, *v*(C-O) 1317,*v*(NN) 1141, *v*(V=O) 974, *v*(VO) 588, *v*(VN) 530. ^{1}H-NMR (400 MHz, DMSO-d_6, ppm): δ = 9.8 (*s*, 1H; *H*C=N), 7.2-8.4 (*m*, 11H; rings), 3.4 (*q*, 2*H*; CH_2), 1.1 (*t*, 4*H*; CH_3).

(2-oxidonaphthalen-1-yl)methylene)benzohydrazonato-propoxido-oxido-vanadium(V) [VO(L)(OPr)] (3)

Yield: 68%. m.p.: 208 °C. Molar Conductance (10^{-3} M, MeOH): 2.9 Ω^{-1} cm^2 mol^{-1}.Anal. Calc. for $C_{21}H_{19}N_2O_4V$ (414.33 g mol^{-1}): C, 60.88; H, 4.62; N, 6.76. Found: C, 60.87; H, 4.71; N, 6.70%. IR (KBr) cm^{-1}: *v*(C=N) 1594, *v*(C=C_{ring}) 1443, *v*(C-O) 1317,*v*(NN) 1136, *v*(V=O)971, *v*(VO)556, *v*(VN)526. ^{1}H-NMR (400 MHz, DMSO-d_6, ppm): δ = 9.8 (*s*, 1H; *H*CH=N), 7.2-8.4 (*m*, 11H; rings), 3.3 (*t*, 2H; CH_2), 1.4 (*m*, 2H; CH_2), 0.8 (*t*, 3H; CH_3).

4.2 Crystal structure determination

The structures were measured using a Gemini diffractometer with an ATLAS CCD detector. Mirror collimated Cu-Kα radiation was used for the ligand **H_2L** and complexes **2** and **3**, while data for complex **1** was collected with graphite monochromated Mo-Kα radiation. Data integration and absorption correction were performed with CrysAlis pro software [48]. The structures were solved using Superflip software[49] and refined with Jana2006[50]. MCE software [51] was used for visualization of the electron density. All hydrogen atoms attached to fully occupied atoms were discernible in difference Fourier maps and could be refined to reasonable geometry. The positions of hydrogen atoms attached to disordered atoms were derived geometrically. According to common practice H atoms bonded to C were kept in ideal positions with C–H = 0.96 Å while positions of H atoms bonded to N and O were refined with restrained bond lengths. In both cases U_{iso}(H) was set to 1.2U_{eq}(C,N,O). All non-hydrogen atoms were refined using harmonic refinement. The disordered solvent molecules were refined with restrained bond lengths. The occupancies of the disorder components were refined with an occupancy sum constrained to 1 for each solvent molecule. For further information on data collection and structure refinement see Table 6.

View Article Online
DOI: 10.1039/C5NJ02594J

Table 6. Crystal data and structure refinement for H_2L and its V(V) complexes.

Compound	**H_2L**	**1**	**2**	**3**
Formula	$C_{18}H_{14}N_2O_2$	$C_{20}H_{19}N_2O_5V$	$C_{20}H_{17}N_2O_4V$	$C_{21}H_{19}N_2O_4V$
M_r	290.3	418.3	400.3	414.3
Crystal system	Monoclinic	Monoclinic	Monoclinic	Monoclinic
Space group	$P2_1/n$	$P2_1/n$	$P2_1/c$	$C2/c$
Radiation	Cu-Kα	Mo-Kα	Cu-Kα	Cu-Kα
λ (Å)	1.54184	0.71073	1.54184	1.5468
T (K)	120	121	120	120
a (Å)	6.9512 (4)	12.7970 (8)	17.8457 (18)	34.6714 (16)
b (Å)	29.5028 (18)	7.8400 (4)	5.9203 (5)	6.0918 (3)
c (Å)	7.4215 (5)	19.3207 (13)	18.1622 (13)	17.8955 (5)
β (°)	108.876 (6)	104.308 (5)	110.679 (8)	97.143 (3)
V (Å^3)	1440.15	1878.3 (2)	1795.2 (3)	3750.4 (3)
Z	4	4	4	8
ρ (g cm^{-3})	1.339	1.479	1.481	1.468
μ (mm^{-1})	0.72	0.56	4.86	4.69
θ_{min}, θ_{max} (°)	6.5, 66.7	3.1, 29.2	4.9, 67.2	5.0, 67.0
Meas. relfns	4356	27921	9573	10825
Uniq. Reflns, R_{int}	2471, 0.026	4751, 0.025	3113, 0.068	3292, 0.056
Params., Restr.	205, 2	260, 3	244, 0	263, 6
R_{all}, $wR2_{all}$	0.043, 0.104	0.038, 0.101	0.070, 0.132	0.060, 0.100
R_{obs}, $wR2_{obs}$	0.036, 0.096	0.032, 0.097	0.051, 0.118	0.039, 0.089
GOF	1.21	1.83	1.28	1.14
$\Delta\rho_{min}$, $\Delta\rho_{max}$ (e Å^{-3})	-0.18, 0.14	-0.36, 0.33	-0.37, 0.63	-0.23, 0.25

4.3 Antimicrobial assays

The antimicrobial activities of the ligand [**H_2L**] and the complexes; [VO(L)(MeOH)(OMe)], [VO(L)(OEt)] and [VO(L)(OPr)] against gram-positive and gram-negative bacteria were evaluated using the agar-well diffusion method. The minimum inhibitory concentrations of all the compounds were also assayed *via* an agar dilution technique.

4.4 Determination of minimum inhibitory concentration (MIC)

In order to determine the MIC of each compound, an agar dilution assay was performed as described previously [52]. Each compound was dissolved in DMSO and mixed well with sterilized, molten Mueller-Hinton agar (45°C) at a 2-fold dilution. Each solution was poured onto a sterile Petri plate to obtain the desired final concentrations (between 19.53 and 5000 μg mL^{-1}) of each compound. Negative (DMSO) control plates with the Mueller-Hinton agar were also prepared.

View Article Online
DOI: 10.1039/C5NJ02594J

The surface of the set agar plates was air-dried under a laminar airflow hood for 30 minutes. One µL of the overnight broth culture of *Escherichia coli* (ATCC 25922) and *Staphylococcus aureus* (ATCC 33591 and 29213), which had been adjusted to 0.5 McFarland-turbidity, was inoculated onto the surface of the plates with different dilutions of the compounds and the inoculum spots allowed to dry at room temperature. All plates were inverted and incubated appropriately for 16-20 hours at 37°C. Each experiment was carried out in triplicate. The minimum inhibitory concentration was defined as the lowest concentration able to inhibit visible bacterial growth on the plates.

4.5 Agar well diffusion assay

Separate samples of cation-adjusted Mueller-Hinton II broth (90922 Fluka) was inoculated with *Escherichia coli* (ATCC 25922) and *Staphylococcus aureus* (ATCC 33591 and 29213) and incubated at 37°C overnight. The microbial turbidity was adjusted equivalent to a 0.5 McFarland turbidity standard. Thereafter, Mueller-Hinton agar plates (Merck, 105437) were swabbed uniformly with the standardized inoculums. Once the surfaces of agar plates were dried aseptically, 6 mm wells were bored using a sterile cork-borer about two cm apart. The bottom of each well was coated with sterilized Mueller-Hinton agar at 45°C. For each microorganism, separate 100 µL samples of the ligand [$\mathbf{H_2L}$], or the V(V) complexes **1**, **2**, and **3** dissolved in DMSO were added into the wells, to provide 500 and 1000 µg of the compound per well, and allowed to diffuse at room temperature for 2 hours. Negative control (DMSO) and positive controls (cefiximetrihydrate, 18588 Fluka, and azithromycin dihydrate, PZ0007 Sigma, 5 and 15 µg/well respectively) were also placed in wells. The plates were incubated face upwards at 37ºC for 24 hours[53]. The diameters of the zones of inhibition were evaluated using a microscope scale. Each experiment was carried out in triplicate.

4.6 Molecular docking

The crystal structure of GlcN-6-P synthase was obtained from the Protein Data Bank (http://www.pdb.org/pdb/home/home.do), PDB ID 2VF5, at a resolution of 2.90 Å [54]. The binding site of the target was selected based on the amino acid residues involved in binding to the glucosamine-6-phosphate of GlcN-6-P synthase as obtained from PDB with ID 2VF5. This would be considered to be the most accurate active region revealed by the experimental crystallographic data. Accordingly, the grid was centered at the region including all the 12 amino

View Article Online
DOI: 10.1039/C5NJ02594J

acid residues surrounding the active site (Ala602, Val399, Ala40 0, Gly301, Thr302, Ser303, Cys300, Gln348, Ser349, Thr352, Ser347 and Lys603). The coordination sphere of ciprofloxacine, as a standard antimicrobial agent and the synthesized ligand and complexes were generated from their X-ray crystal structure as a CIF file. Mercury software (http://www.ccdc.cam.ac.uk/) was then used to convert the CIF files to PDB format [55]. Finally, molecular docking studies were carried out using Autodock 4.2.5 software [56] with the grid box size set at 70, 64, and 56 Å for x , y and z, respectively, and the grid center set at 30.59, 15.822 and 3.497 for x , y and z, respectively. All molecular images and animations were produced using the Discovery Studio Visualizer 4.5 package.

5. Supplementary data

CCDC 1062415, 1062606, 1062416, and 1062417 contains the supplementary crystallographic data for H_2L, **1**, **2** and **3** respectively. A copy of this information may be obtained free of charge from The Director, CCDC, 12 Union Road, Cambridge, Cb2 1EZ, UK (fax: +44 1223 336 033); web page: http://www.ccdc.cam.ac.uk/cgibin/catreq.cgi

6. Acknowledgements

Authors gratefully acknowledge the financial support provided for this work by the Shahid Bahonar University of Kerman. JS thanks the Chemistry Department, University of Otago for support of his work. The crystallographic part was supported by the project 15-12653S of the Czech Science Foundation using instruments of the ASTRA lab established within the Operation program Prague Competitiveness - project CZ.2.16/3.1.00/24510

References

1. P. Melnyk, V. Leroux, C. Sergheraert and P. Grellier, *Bioorg. Med. Chem. Lett.*, 2006, **16**, 31-35.
2. P. Crisalli and E. T. Kool, *J. Org. Chem.*, 2013, **78**, 1184-1189.
3. R. Takjoo, J. T. Mague, A. Akbari and S. Y. Ebrahimipour, *J. Coord. Chem.*, 2013, **66**, 2852-2862.
4. S. Y. Ebrahimipour, J. T. Mague, A. Akbari and R. Takjoo, *J. Mol. Struct.*, 2012, **1028**, 148-155.

View Article Online
DOI: 10.1039/C5NJ02594J

5. D. Rehder, *Bioinorganic Vanadium Chemistry*, Wiley, 2008.
6. D. Rehder, *Angew. Chem. Int. Ed. Engl.*, 1991, **30**, 148-167.
7. N. D. Chasteen, in *Copper, molybdenum, and vanadium in biological systems*, Springer, 1983, pp. 105-138.
8. R. R. Eady, *Coord. Chem. Rev.*, 2003, **237**, 23-30.
9. D. Rehder, G. Santoni, G. M. Licini, C. Schulzke and B. Meier, *Coord. Chem. Rev.*, 2003, **237**, 53-63.
10. A. Sigel and H. Sigel, *Metal Ions in Biological Systems: Volume 31: Vanadium and its Role for Life*, Taylor & Francis, 1995.
11. G. L. Mendz, *Arch. Biochem. Biophys.*, 1991, **291**, 201-211.
12. A. S. Tracey and D. C. Crans, *Vanadium compounds: chemistry, biochemistry, and therapeutic applications*, Amer Chemical Society, 1998.
13. D. Rehder, *Coord. Chem. Rev.*, 1999, **182**, 297-322.
14. Z. H. Chohan, S. H. Sumrra, M. H. Youssoufi and T. B. Hadda, *Eur. J. Med. Chem.*, 2010, **45**, 2739-2747.
15. S. Y. Ebrahimipour, I. Sheikhshoaie, A. Crochet, M. Khaleghi and K. M. Fromm, *J. Mol. Struct.*, 2014, **1072**, 267-276.
16. C. Bates and C. Pasternak, *Biochem. J.*, 1965, **96**, 147-154.
17. H. Chmara, R. Andruszkiewicz and E. Borowski, *BBA-Protein Struct. M.*, 1986, **870**, 357-366.
18. P. Shyma, B. Kalluraya, S. Peethambar, S. Telkar and T. Arulmoli, *Eur. J. Med. Chem.*, 2013, **68**, 394-404.
19. G. Jose, T. S. Kumara, G. Nagendrappa, H. Sowmya, J. P. Jasinski, S. P. Millikan, N. Chandrika, S. S. More and B. Harish, *Eur. J. Med. Chem.*, 2014, **77**, 288-297.
20. S. Y. Ebrahimipour, I. Sheikhshoaie, M. Mohamadi, S. Suarez, R. Baggio, M. Khaleghi, M. Torkzadeh-Mahani and A. Mostafavi, *Spectrochim. Acta, Part A*, 2015, **142**, 410-422.
21. S. Y. Ebrahimipour, I. Sheikhshoaie, J. Castro, W. Haase, M. Mohamadi, S. Foro, M. Sheikhshoaie and S. Esmaeili-Mahani, *Inorg. Chim. Acta*, 2015, **430**, 245-252.
22. S. Y. Ebrahimipour, I. Sheikhshoaie, A. C. Kautz, M. Ameri, H. Pasban-Aliabadi, H. Amiri Rudbari, G. Bruno and C. Janiak, *Polyhedron*, 2015, **93**, 99-105.
23. R. Takjoo, A. Akbari, S. Y. Ebrahimipour, H. Amiri Rrudbari and Giuseppe Brunò, *C. R. Chim.*, 2014, **17**, 1144-1153.
24. S. Y. Ebrahimipour, H. Khabazadeh, J. Castro, I. Sheikhshoaie, A. Crochet and K. M. Fromm, *Inorg. Chim. Acta*, 2015, **427**, 52-61.
25. S. Y. Ebrahimipour, M. Mohamadi, J. Castro, N. Mollania, H. Amiri Rudbari and A. Saccá, *J. Coord. Chem.*, 2015, **68**, 632-649.
26. S. Y. Ebrahimipour, M. Abaszadeh, J. Castro and M. Seifi, *Polyhedron*, 2014, **79**, 138-150.
27. A. Sundar, M. Prabhu, N. Indra Gandhi, M. Marappan and G. Rajagopal, *Spectrochim Acta A*, 2014, **129**, 509-518.
28. S. T. Chew, K. M. Lo, S. K. Lee, M. P. Heng, W. Y. Teoh, K. S. Sim and K. W. Tan, *Eur. J. Med. Chem.*, 2014, **76**, 397-407.
29. F. H. Allen, O. Kennard, D. G. Watson, L. Brammer, A. G. Orpen and R. Taylor, *J. Chem. Soc., Perkin Trans. 2*, 1987, S1-S19.
30. Y. Qiao, X. Ju, Z. Gao and L. Kong, *Acta Crystallogr. Sect. Sect. E: Struct. Rep. Online*, 2009, **66**, o95-o95.

View Article Online
DOI: 10.1039/C5NJ02594J

31. C. R. Groom and F. H. Allen, *Angew. Chem. Int. Ed.*, 2014, **53**, 662-671.
32. S. Y. Liu, S. S. Sun, T. T. Zheng, X. L. Zheng, X. F. Zhao and X. F. Li, *Acta Crystallogr. Sect. Sect. E: Struct. Rep. Online*, 2011, **67**, 965-965.
33. Y. G. Zhao, B. G. Zhang, C.-Y. Duan, Z. H. Lin and Q. J. Meng, *New J. Chem.*, 2006, **30**, 1207-1213.
34. A. L. Spek, *Acta Crystallogr. Sect. D. Biol. Crystallogr.*, 2009, **65**, 148-155.
35. J. H. Liu, Q. Z. Zhang, X. He, W. B. Yang and C. Z. Lu, *Chinese J. Inorg. Chem.*, 2006, **6**, 1028-1032.36. a) F.-M. Wang, *Acta Crystallogr. Sect. Sect. E: Struct. Rep. Online*, 2011, **67**, 1254-1254; b) N. Wang, J. Guo and J. Hu, *Russ. J. Coord. Chem.*, 2013, **39**, 891-895; c) N. A. Lalami, H. H. Monfared, H. Noei and P. Mayer, *Transition Met. Chem.*, 2011, **36**, 669-677; d) C. Y. Wang, J. J. Hu, H.-Y. Tu, P. F. Zhu and S. J. Sheng, *Acta Crystallogr. Sect. Sect. E: Struct. Rep. Online*, 2011, **67**, 1475-1476.
37. A. W. Addison, T. N. Rao, J. Reedijk, J. Van Rijn and G. C. Verschoor, *J. Chem. Soc., Dalton Trans.*, 1984, 1349-1356.
38. Y. Qing, L. Chun-Ying, B. He-Dong, L. Hong, S. Hai-Bin and W. Hong-Gen, *Chin. J. Struct. Chem.*, 2007, **26**.
39. J. Bernstein, R. E. Davis, L. Shimoni and N. L. Chang, *Angew. Chem. Int.l Ed. Engl.*, 1995, **34**, 1555-1573.
40. L. M. Salonen, M. Ellermann and F. Diederich, *Angew. Chem. Int. Ed.*, 2011, **50**, 4808-4842.
41. R. Papadakis, E. Rivière, M. Giorgi, H. Jamet, P. Rousselot-Pailley, M. Reglier, A. J. Simaan and T. Tron, *Inorg. Chem.*, 2013, **52**, 5824-5830.
42. H. Khaledi, M. M. Olmstead, H. Mohd Ali and N. F. Thomas, *Inorg. Chem.*, 2013, **52**, 1926-1941.
43. Z.-L. You, D.-H. Shi, J.-C. Zhang, Y. P. Ma, C. Wang and K. Li, *Inorg. Chim. Acta*, 2012, **384**, 54-61.
44. P. Plitt, H. Pritzkow and R. Krämer, *Dalton Trans.*, 2004, 2314-2320.
45. H.-M. Liu, J.-M. Wang, D.-N. Zhang, P. L. Cui and J. J. Ma, *Synth. React. Inorg. Met. Org. Chem.*, 2013, **43**, 1251-1255.
46. a) B. Mondal, M. G. Drew, R. Banerjee and T. Ghosh, *Polyhedron*, 2008, **27**, 3197-3206; b) M. Sutradhar, T. R. Barman, G. Mukherjee, M. G. Drew and S. Ghosh, *Polyhedron*, 2012, **34**, 92-101.
47. T. D. Thangadurai and K. Natarajan, *Transit. Metal Chem*, 2001, 26(4-5), 500–504.
48. CrysAlis, *Oxfordshire, England*, 2012.
49. L. Palatinus and G. Chapuis, *J. Appl. Crystallogr.*, 2007, **40**, 786-790.
50. V. Petricek, M. Dusek and L. Palatinus, *Z. Kristallogr.*, 2014, **229(5)**, 345-352..
51. J. Rohlíček and M. Hušák, *J. Appl. Crystallogr.*, 2007, **40**, 600-601.
52. I. Wiegand, K. Hilpert and R. E. Hancock, *Nat. Protoc.*, 2008, **3**, 163-175.
53. A. Sen and A. Batra, *Int. J. Curr. Pharm. Res.*, 2012, **4**, 67-73.
54. S. Mouilleron, M. A. Badet-Denisot and B. Golinelli-Pimpaneau, *J. Mol. Biol.*, 2008, **377**, 1174-1185.
55. C. F. Macrae, I. J. Bruno, J. A. Chisholm, P. R. Edgington, P. McCabe, E. Pidcock, L. Rodriguez-Monge, R. Taylor, J. V. Streek and P. A. Wood, *J. Appl. Crystallogr.*, 2008, **41**, 466-470.
56. G. M. Morris, R. Huey, W. Lindstrom, M. F. Sanner, R. K. Belew, D. S. Goodsell and A. J. Olson, *J. Comput. Chem.*, 2009, **30**, 2785-2791.

View Article Online
DOI: 10.1039/C5NJ02594J

Antimicrobial activity of arylhydrazone-based oxido vanadium(V) complexes: *in-vitro* and *in silico* studies

S. Yousef Ebrahimipour*, Iran Sheikhshoaie, Jim Simpson, Hadi Ebrahimnejad, Michal Dusek, Nima Kharazmi, Vaclav Eigner

A series of oxido vanadium(V) complexes have been synthesized and evaluated from the point of experimental and theoretical antimicrobial activity.